ANNUAL REVIEWS

Annual Review of Analytical Chemistry

Wearable Sensors for Biochemical Sweat Analysis

Amay J. Bandodkar,[1,2,*] William J. Jeang,[1,2,*] Roozbeh Ghaffari,[2,3,4] and John A. Rogers[1,2,4–8]

[1]Department of Materials Science and Engineering, Northwestern University, Evanston, Illinois 60208, USA; email: jrogers@northwestern.edu

[2]Center for Bio-Integrated Electronics, Simpson Querrey Institute for BioNanotechnology, Northwestern University, Evanston, Illinois 60208, USA

[3]Epicore Biosystems, Inc., Evanston, Illinois 60208, USA

[4]Department of Biomedical Engineering, Northwestern University, Evanston, Illinois 60208, USA

[5]Department of Materials Science and Engineering, University of Illinois at Urbana-Champaign, Urbana, Illinois 61801, USA

[6]Frederick Seitz Materials Research Laboratory, University of Illinois at Urbana-Champaign, Urbana, Illinois 61801, USA

[7]Feinberg School of Medicine, Northwestern University, Evanston, Illinois 60208, USA

[8]Departments of Electrical Engineering and Computer Science, Neurological Surgery, Chemistry, and Mechanical Engineering, Northwestern University, Evanston, Illinois 60208, USA

Annu. Rev. Anal. Chem. 2019. 12:1–22

First published as a Review in Advance on February 20, 2019

The *Annual Review of Analytical Chemistry* is online at anchem.annualreviews.org

https://doi.org/10.1146/annurev-anchem-061318-114910

*These authors contributed equally to this article.

Keywords

wearable sensors, biosensors, sweat analysis, health monitoring, microfluidics

Abstract

Sweat is a largely unexplored biofluid that contains many important biomarkers ranging from electrolytes and metabolites to proteins, cytokines, antigens, and exogenous drugs. The eccrine and apocrine glands produce and excrete sweat through microscale pores on the epidermal surface, offering a noninvasive means for capturing and probing biomarkers that reflect hydration state, fatigue, nutrition, and physiological changes. Recent advances in skin-interfaced wearable sensors capable of real-time in situ sweat collection and analytics provide capabilities for continuous biochemical monitoring in an ambulatory mode of operation. This review presents a broad overview of sweat-based biochemical sensor technologies with an emphasis on enabling materials, designs, and target analytes of interest. The article concludes with a summary of challenges and opportunities for researchers and clinicians in this swiftly growing field.

1. INTRODUCTION

Wearable sensors that interface directly with the skin represent an emerging class of technology that enables unique modes of continuous, noninvasive monitoring with relevance across many applications in personalized medicine, athletic performance, and military readiness (1–6). The soft physical construction and thin, lightweight designs of these skin-interfaced systems are essential defining characteristics that underpin their utility. As such, these devices embody significant, qualitative advances over the types of wired, bulky diagnostic instruments found in hospital and laboratory settings and over conventional, wrist-mounted wearables. In the skin-integrated systems highlighted in this review, onboard electronics, sensors, power supplies, and data communication systems facilitate continuous and comprehensive, real-time clinical-grade health monitoring outside of controlled settings. In the field of biomedicine, the resulting capabilities have the potential to fundamentally transform strategies for patient monitoring and treatment. A resulting surge in academic and industrial research in this area aimed at tracking body movements (7, 8), temperature (9, 10), cardiac activity [electrocardiography, ECG (11, 12)], brain processes [electroencephalography, EEG (13)], muscle contractions [electromyography, EMG (14, 15)], electrical and thermal properties (16), hemodynamics (17, 18), blood pressure (12), and others. Although these biophysical parameters provide invaluable insights into physiological status, they lack direct information on dynamic biochemical and metabolic processes.

Biochemical sensors that noninvasively analyze biofluids like saliva, sweat, tears, and interstitial fluids offer the potential to radically improve assessment of health status by tracking changes in metabolic processes (19). Sweat is particularly attractive due to its ease of collection and presence of biomarkers related to important health conditions such as dehydration, physical fatigue, mental stress, and disease (20–22). Collection of sweat samples most typically relies on absorbent pads or plastic microtubes (Macroduct Sweat Collection System) strapped to the skin and using traditional laboratory instruments for chemical evaluation (23). However, these methods are incompatible with remote monitoring, continuous assessment, or use in the field due to their reliance on cumbersome, multistep procedures for sample preparation and expensive, benchtop hardware for analysis.

Recent advances in soft microfluidics, flexible/stretchable electronics, and chemical sensing techniques serve as the foundations for novel skin-mounted systems that overcome key limitations of conventional approaches. This review focuses on the rapidly growing field of wearable biochemical sweat sensors as a promising direction for continuous health and physiological monitoring. The content includes summaries of key wearable device technologies for field studies and practical applications outside of labs and clinics across multiple targets for biochemical sensing. A concluding section discusses technical challenges and future directions in these types of wearable metabolic device platforms.

2. ENABLING MATERIALS AND TECHNOLOGIES

Precise measurements of sweat dynamics (i.e., rate and local loss) and sweat biomarkers require advanced classes of wearable chemical systems capable of directly interfacing with the skin for the continuous capture and analysis of sweat and for transmission of the resulting information in real time, locally to the user and/or remotely to health professionals. In this section, we review various demonstrated biosensor modalities, electronics modules, wireless communication strategies, and soft mechanical designs for systems having these functional capabilities.

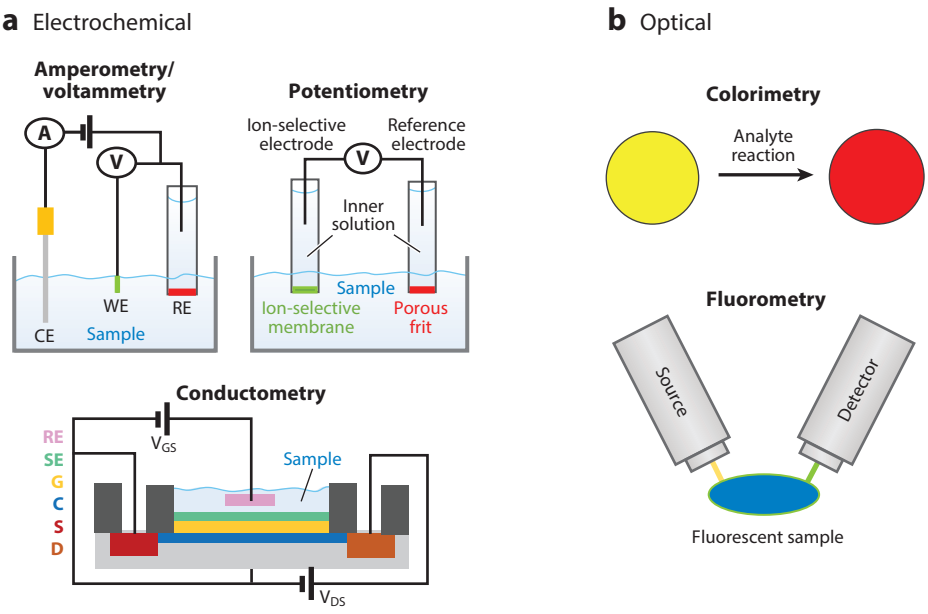

Figure 1

Sensing modalities. Schemes illustrating (*a*) electrochemical and (*b*) optical techniques. Abbreviations: A, ammeter; C, channel; CE, counter electrode; D, drain; G, gate; RE, reference electrode; S, source; SE, sensing element; V, voltmeter; V_{DS}, voltage across source and drain; V_{GS}, voltage across gate and source; WE, working electrode.

2.1. Sensing Modalities

Key requirements for skin-interfaced sweat sensors include fast response times, high sensitivity and selectivity, stability under various environmental conditions, and power efficient operation. Several electrochemical (**Figure 1*a***) and optical (**Figure 1*b***) technologies satisfy these criteria, at least in part. Electrical approaches such as amperometry, potentiometry, voltammetry, and conductometry offer relevant sensing capabilities. Advances in nanomaterials and surface functionalization processes (24–27) allow for miniaturized devices with highly sensitive measurements of such species at low concentrations typical of sweat (28, 29). Amperometry is well suited for detecting a range of metabolites since many of these analytes readily undergo redox reactions in the presence of inorganic and/or biological catalysts at potentials below that necessary for electrolysis of water. As with conventional approaches, wearable amperometric sensors include a working electrode, where the analyte undergoes an electrochemical reaction; a reference electrode for defining a fixed potential at the working electrode; and a counter electrode that serves as a current collector. Existing devices rely on either the consumption of dissolved oxygen and production of hydrogen peroxide during the enzymatic reaction (first-generation enzymatic biosensor) or the oxidation/reduction of artificial mediators (second-generation enzymatic biosensor) or nanomaterials (third-generation enzymatic biosensor) that transport electrons between enzyme active sites and the electrode. Potentiometry allows detection of electrolytes, where the standard redox potentials exceed that of water electrolysis. A generic potentiometric sensor includes an ion-selective electrode and a reference electrode. The potential of the reference electrode is independent of the sample composition, while that of the ion-selective electrode follows the Nernst equation and depends on the activity of the analyte ion and, hence, indirectly on its concentration.

Progress in electrode materials in the form of conducting polymers (30) and nanomaterials (31) renders all solid-state ion-to-electron transducers as highly sensitive, small-scale, ion-selective electrodes that can be integrated into wearable platforms. Voltammetry is most relevant for rapid, multianalyte detection of minerals (32–34), drugs (35–37), pollutants (38), and other target species. Similar to amperometry, voltammetric sensors have a three-electrode configuration, but unlike the former, the potential is scanned within a range to oxidize/reduce the analyte(s). The amplitudes of local maxima in the measured current depend on analyte concentrations. In addition to the active materials, the voltage waveforms, step sizes, frequencies, and amplitudes are important parameters which, when optimized, can support detection of multiple analytes at concentrations of parts per million or even parts per trillion levels. Conductometric approaches typically take the form of chemical field-effect transistors, of interest partly due to their scalability and natural compatibility with complementary metal-oxide semiconductor (CMOS) technologies. Such sensors consist of source and drain electrodes with a semiconducting material in between and a capacitively coupled gate electrode. The gate is designed to be chemically sensitive to the analyte such that interaction between the analyte and the gate electrode modulates the gate potential, which in turn leads to measurable changes in the conductivity of the channel. However, reliance on bulky complex electronics and relatively high-capacity power supplies often limits the utility of such electrochemical transducers in skin-mounted platforms for remote settings.

Optical transducers in the form of colorimetric or fluorometric assays offer analysis capabilities that bypass such disadvantages. Here, chemical reactions and/or interactions induced by the analytes produce quantifiable changes in optical wavelength or intensity, typically in the visible range. Their simple, low-cost construction and ability to operate without electrical power in thin, lightweight designs match well to form factor requirements of skin-mounted wearables. These attributes, together with options for visual readout for semiquantitative evaluation, and color extraction from digital images (smartphones, digital camera) for quantitative analysis make them attractive for biomedical (39, 40), environmental (41), and security (42) applications in limited-resource settings. Emerging classes of colorimetric and fluorometric probes, the latter of which can also be configured for readout using a smartphone configured with simple plug-in modules, utilize organic dyes (43), quantum dots (44), and metal nanoparticles (45) as high-performance, inexpensive, simple sensing platforms for analysis of complex matrixes that are compatible with wearable technology. Reports of wearable devices that exploit such optical approaches can detect glucose, lactate, chloride, pH, zinc, and sodium (46–49).

2.2. Substrates and Encapsulating Materials

Materials such as silicon, fiberglass composites, and glass employed in conventional electronics and electrochemical sensors embody rigid (moduli of 10^9–10^{12} Pa), planar, and brittle physical properties. The human epidermis, by contrast, is soft (moduli of $\sim 10^5$–10^6 Pa), curvilinear, and deformable (50). This inherent mechanical mismatch often causes irritation, discomfort, poor signal quality, and mechanical failure in wearable devices designed for efficient collection and reliable analysis of sweat. Advanced mechanics principles, soft encapsulating materials, and compliant substrates thus play crucial roles in realizing acceptable comfort, signal quality, and watertight interfaces to the skin.

Materials with relatively low Young's moduli (10^6–10^{12} Pa range), such as flexible plastics, fabrics, and elastomers, serve as suitable substrates, encapsulating layers, and skin adhesives in wearable sensors. Although the elastic moduli of most polymers ($>10^9$ Pa range) do not align with those of skin, their low flexural rigidity in thin-film forms, broad range of low-cost biocompatible formulations, optical transparency, and chemical inertness lead to widespread use in various types of

Figure 2

Encapsulating materials and substrates. (*a*) Examples of flexible plastic-based sensors. Adapted with permission from Reference 53; copyright 2016, Nature Publishing Group; Reference 51, copyright 2016, Nature Publishing Group; Reference 52, copyright 2017, American Chemical Society; Reference 54, copyright 2014, American Chemical Society. (*b*) Examples of fabric-based sensors. Adapted with permission from Reference 57, copyright 2016, Wiley; Reference 58, copyright 2016, Elsevier; Reference 59, copyright 2012, Royal Society of Chemistry; Reference 60, copyright 2016, Royal Society of Chemistry. (*c*) Examples of elastomer-based sensors. Adapted with permission from Reference 93, copyright 2016, Nature Publishing Group; Reference 90, copyright 2018, American Chemical Society; Reference 46, copyright 2016, AAAS; Reference 62, copyright 2015, American Chemical Society.

wearable sensors (**Figure 2*a***). Polyethylene terephthalate (PET), polyimide (PI), polyester (PE), and inkjet temporary tattoo paper (thin, flexible plastic membrane on releasable backing paper) are specific examples of plastics that support wearable flexible sensors (51–55). Their compatibility with additive patterning techniques such as inkjet and screen printing represents a further notable attribute. However, their poor breathability and inability to stretch to accommodate the natural motions of the skin restrict practical use of such substrates to miniaturized layouts and applications that require only brief time durations on the skin.

Fabrics, by contrast, are much more compliant and breathable than polymer films. The diverse array of fibers and weave patterns, low costs per unit area of fabrics, and widespread use in clothing yield a class of sensor substrates that allows for seamless integration of devices into apparel as discreet components or functional fashion. Clothing fabrics accommodate large area interfaces with the skin, with many options in sweat collection and handling. Fabrics are hierarchal composite

materials composed of yarns that consist of even smaller fibers. Fiber materials and processing approaches define the chemical structures, mechanical properties, and specific surface areas of fabrics as essential parameters in developing robust wearable sensors. A large library of natural (e.g., cotton, silk, wool) and synthetic (e.g., nylon, polyester, carbonaceous materials, spandex) fibers supports a variety of tailorable surface chemical functional groups for enhanced sensor functionality. Furthermore, the degree of twisting of fibers within yarns and the spinning of these yarns into knitted, woven, or nonwoven forms modulate the mechanical resiliency and effective surface area (56). Two major approaches in fabric-based wearable sensors include (*a*) direct fabrication/integration of sensors onto fabric surfaces (57–59) and (*b*) formation of yarn-based sensors that can be processed to form the fabrics themselves (60). The first scheme involves transfer printing of fully formed sensors onto commercially available fabrics or direct printing of functional materials onto fabrics in a layer-by-layer fashion to fabricate surface-mounted sensors. A challenge in this latter option is that the high roughness, porosity, and wicking properties of the fabric can lead to poor adherence and/or quality of the printed materials. These issues can be addressed by applying a thin stretchable elastomer base layer onto the fabric prior to printing to yield a smooth, well-controlled surface (61). The latter option simply involves integration of the preformed yarn-based sensors into the fabric. These two approaches support a wide range of wearable colorimetric and electrochemical sensors on a variety of fabrics such as cotton, polyester, Gortex, nylon, and spandex (**Figure 2*b***).

Although fabrics represent an interesting class of substrate materials, disadvantages include a relative lack of intimate watertight skin contact, limited stretchability, and low chemical resistance. Thin, low-modulus, biocompatible elastomers represent nearly ideal classes of materials. Examples include silicones (62), polyurethanes, and copolymers (e.g., styrene-butadiene-styrene block copolymer). Careful selection of chemical building blocks, degrees of cross-linking, and ratios of hard and soft components yield a range of materials that can support mechanical properties and water/vapor permeabilities specifically tailored to the skin (63). Choices of oligomer composition and side-chain moieties provide additional mechanisms for control over mechanical and chemical properties (64). Additionally, bioinspired composites of carefully designed thin, filamentary mesh structures embedded into elastomeric substrates yield systems with stress-strain responses that can be tailored to mimic the full "J-shaped" stress-strain response of human skin (65). The filamentary structures allow stretchability, with an intrinsic strain-limiting mechanism for protecting biological tissues and the device from excessive deformation. Adhesion characteristics are particularly important for efficient collection of sweat without leakage at the skin interface or delamination. Surface and chemical modifications, addition of surfactants, and blends with hydrophilic polymers are important in this context, where strategies established in the skin bandage industry are widely applicable. As with the other options, fabrication of sensors on elastomeric substrates can involve transfer or direct printing (**Figure 2*c***).

2.3. Soft Microfluidic Systems

The human epidermis contains ~200 eccrine glands/cm^2 over much of the body (66) with densities that vary significantly across various anatomical regions (67). The average rates of generation and release of sweat from these glands can vary by orders of magnitude, depending on heat acclimatization (68), age (69), diet (70), environmental conditions (71), and physiological state (72, 73). Wearable sweat sensors must perform sweat analytics over this large range of rates of sweating and across multiple body positions. Recent studies demonstrate sophisticated microfluidic systems rendered in thin, soft, skin-compatible forms to facilitate capture of sweat directly from the skin as it emerges through pores, and transport through valves, separators, and reservoirs for analysis. Well-defined inlet(s) on the skin-interfaced side of these microfluidic systems enable operation at

precise locations of the skin in ways that allow quantitation of spatial variations in sweat rate, loss, and chemistry. These platforms isolate the sweat from the skin immediately as it emerges from the surface to yield pristine samples for onboard analysis. Their constructions additionally encapsulate and protect sensors from biofouling due to debris and oils on the skin surface and from environmental contaminants. Low-signal noise levels follow from the guiding of irregular sweat flows from the skin surface into laminar channels prior to interaction with the sensors. Advanced microfluidic designs, adaptable from concepts developed in the lab-on-a-chip community, exploit complex valving, handling, mixing, and routing strategies to direct sweat to multiple isolated sensing regions, thereby reducing cross talk and associated sensing errors (74).

These skin-interfaced systems leverage standard processes in microfluidics fabrication, but instead of hard plastics and glass materials, they consist entirely of low-modulus elastomers capable of comfortable, nonirritating watertight seals to the skin. Specific design strategies for inlet/outlet dimensions, channel geometries, adhesive interfaces, and materials selections are crucial to ensure that natural eccrine gland sweat pressures are sufficient for driving sweat throughout the device (46). Additionally, the geometric adhesive layouts must be carefully designed to avoid, or amplify, compensatory sweating effects that can dramatically increase local rates of sweat release into the inlets. For colorimetric or fluorometric analysis approaches, the top layers of the devices must have sufficient transparency to enable optical inspection (47, 49).

Basic wearable microfluidic designs utilize direct channels from the inlets to single reaction reservoirs for colorimetric or electrochemical sensing (**Figure 3*a–f***) (46, 75, 76). Many colorimetric assays undergo irreversible color changes, limiting such devices to single time-point analysis. Electrochemical sensors provide real-time analysis due to their reversible nature but require costly and bulky power sources and electronics for data logging. More advanced microfluidic systems, featuring multiple reaction chambers separated by using various passive valving technologies, can track time-dependent changes in biomarker concentrations with colorimetric approaches. These layouts accommodate irreversible chemical sensing while mitigating cross talk between different assays. Additionally, calibrated markers along microfluidic channels reveal sweat dynamics as defined by instantaneous sweat rate and total sweat loss.

One approach for multichamber chronometric sweat sampling utilizes hydrophobic and superabsorbent valves within microfluidic channels to guide incoming sweat through several, sequential sets of reaction zones (**Figure 3*g***) (47). Here, a single set includes three distinct reaction zones that each contain an irreversible chloride detection assay optimized for a different concentrations range (0–75 mM, 75–150 mM, and >150 mM). Hydrophobic patterned microchannels act as valves to divert sweat toward the first set of reaction zones for initial chloride measurement. Upon complete filling, a superabsorbent polymer (formed by gelation and subsequent drying of sodium polyacrylate and *N*,*N*′-methylenebisacrylamide in the presence of sodium metabisulfite) at the inlet of each reaction zone expands and blocks sweat flow, thereby acting as a valve to isolate the reaction zone (**Figure 3*h***). This scheme reduces assay-to-assay cross contamination and facilitates buildup of fluidic pressure needed to overcome the hydrophobic valve to route sweat to the next set of assays. This mechanism is the basis of a dynamic fluid guiding system for sequential filling and time-sequenced chloride analysis, but it is applicable to any type of assay.

An alternative means to similar functionality exploits a passive system of capillary burst valves (CBVs). Here, the lithographically defined geometries of the valves result in bursting pressures that lie in ranges compatible with those generated by eccrine glands (77, 78). As a rule of thumb, decreasing the width of the valve and increasing the angle of the outlet increase the bursting pressure. One reported device incorporates CBVs located at the junctions between connecting microfluidic channels and the inlets of various reaction chambers (**Figure 3*i***). A single junction incorporates a first CBV (CBV #1) positioned along the microchannel with a bursting pressure

Single reaction zone

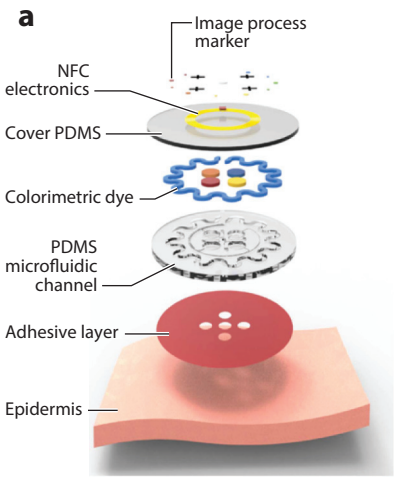

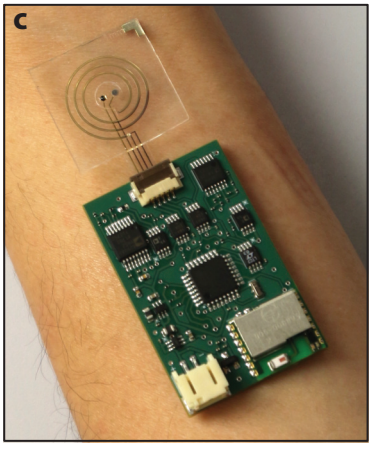

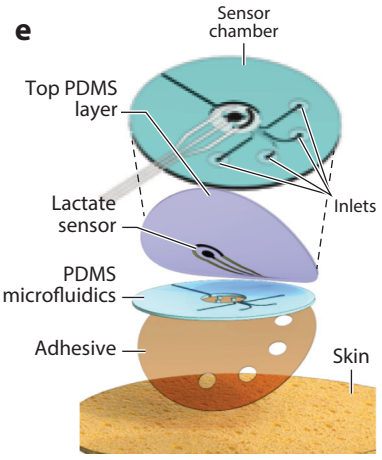

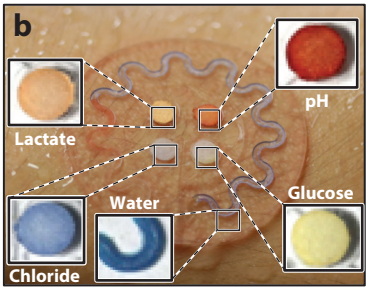

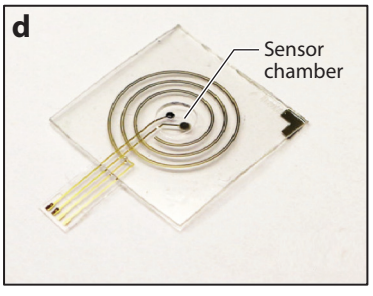

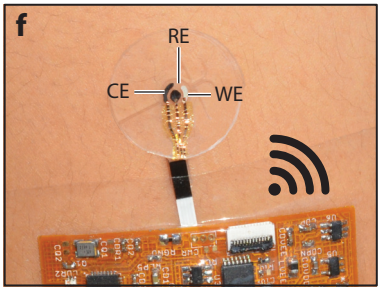

Multiple reaction zones

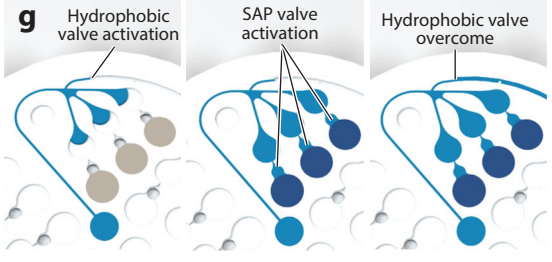

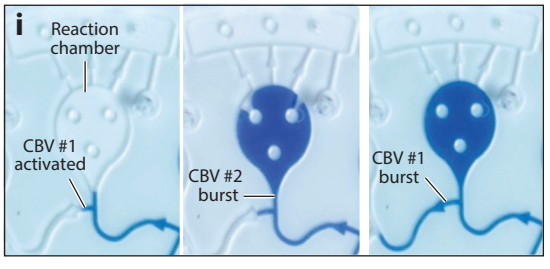

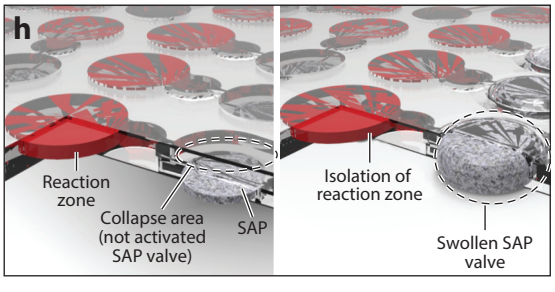

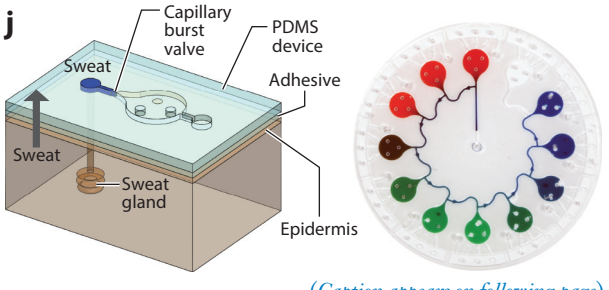

(*Caption appears on following page*)

Figure 3 (*Figure appears on preceding page*)

Soft microfluidic-based chemical sensors. (*a*) Exploded view schematic illustration of a silicone-based microfluidic platform for multianalyte colorimetric sensing. (*b*) Image of the actual device on a human subject. Adapted with permission from Reference 46. Copyright 2016, AAAS. (*c*) Image of an electrochemical sodium sweat sensor with a microfluidic channel for simultaneous sweat rate monitoring. (*d*) Photograph of the microfluidics system. Adapted with permission from Reference 75. Copyright 2018, American Chemical Society. (*e*) Schematic illustration and (*f*) image of an electrochemical lactate sensor embedded within a soft microfluidics system with multiple inlets for rapid sweat sensing. Adapted with permission from Reference 76. Copyright 2017, American Chemical Society. (*g*,*h*) Schematic illustrations of hydrophobic and superabsorbent valves and their function within a wearable microfluidics system for time-sequenced sampling and chemical sensing. Adapted with permission from Reference 47. Copyright 2018, Wiley. (*i*,*j*) Images and schematic illustrations of passive CBVs within a soft wearable microfluidics system and their working principle for chrono-sampling and capture of sweat. Panel *i* adapted with permission from Reference 77, copyright 2017, Wiley; panel *j* adapted with permission from Reference 78, Copyright 2017, Royal Society of Chemistry. Abbreviations: CBV, capillary burst valve; CE, counter electrode; NFC, near-field communications; PDMS, polydimethylsiloxane; RE, reference electrode; SAP, superabsorbent polymer; WE, working electrode.

larger than that of a second CBV (CBV #2) located at the inlet of the reaction chamber. This difference in bursting pressure leads to complete filling of the reaction chamber before the flow can generate sufficient pressure to burst CBV #2, thereby allowing sweat to pass to the next junction. By this process, the device is capable of collecting, storing, and analyzing sweat samples in a chronometric fashion (**Figure 3*j***).

2.4. Power and Data Acquisition

Electrochemical sensors represent the majority of wearable chemical sensors reported to date, making power sources essential components in wearable sensor systems. Power source specifications primarily depend upon the power requirements of the sensor, sampling rate, and the employed communications protocol. Demonstrated wearable sensors largely rely on commercial batteries (53, 79, 80). Although these components increase the device footprint and weight, they provide reliable uninterrupted power supply for continuous data acquisition. Bluetooth low energy (BLE) (80) technology conveniently provides long-distance continuous wireless data transfer from the device to a receiving station up to 30 m away. This makes BLE-based devices attractive for applications requiring long-range data reading. A major drawback, however, is the large power consumption of BLE modules. On the other hand, devices incorporating near-field communications (NFCs) utilize much simpler electronics and close vicinity readers to allow for completely battery-free designs (81). This technology effectively decreases overall electronics footprint and power consumption. NFC-based devices thus find greater utility in applications involving athletes or infants where obtrusive devices may interfere with performance or result in significant burden.

3. KEY TARGETS

The rich milieu of electrolytes, metabolites, vitamins, amino acids, minerals, and various small molecules (29) found in sweat offers potential insights into different aspects of human metabolic and physiological status. For instance, sweat glucose (82–84), ethanol (85, 86), chloride (79), sodium (87), cortisol (88), and lactate (89) levels provide information on glycemic conditions, stress, physical fatigue, and dehydration. Unlike traditional benchtop analyzers, wearable devices offer unprecedented real-time access to monitor these and other conditions. The following subsections describe the key sweat biomarker targets and associated state-of-the-art wearable sensor platforms.

3.1. Metabolites

Significant interest in sweat lactate and glucose stems from their correlations to muscle fatigue (89) and blood glucose levels (90), respectively. Most efforts to develop metabolic sensors employ amperometry (51), although some work focuses on colorimetric assays (46) and electrochemical transistors (91). The fabrication approaches leverage screen printing (92), lithography (93), and vacuum filtration techniques, and/or transfer printing (90) processes to realize device layouts. Subsequent functionalization of the working electrodes with enzymes and other reagents imparts selectivity and enables high sensitivity.

Although nearly all reported wearable metabolic sensors rely on enzymes for selectivity, the labile nature of these biorecognition elements causes performance degradation over time and under different environmental conditions. Recent efforts that involve nonenzymatic sensing approaches (e.g., for glucose) attempt to address this issue by exploiting selective glucose oxidation properties of cobalt wolframate ($CoWO_4$) (90). Here, vacuum-filtered gold nanosheets transferred onto silicone sheets provide the foundations for sensors that can operate even under mechanical strains of 30% (**Figure 4*a***). Surface modification of these nanosheets with alternating layers of positively and negatively charged carbon nanotubes (CNTs) increases surface area and sensitivity. Subsequent dip coating of $CoWO_4$/CNT composite (**Figure 4*b***) functionalizes the working electrode for selective, nonenzymatic glucose detection with a linear sensing range up to at least 0.3 mM

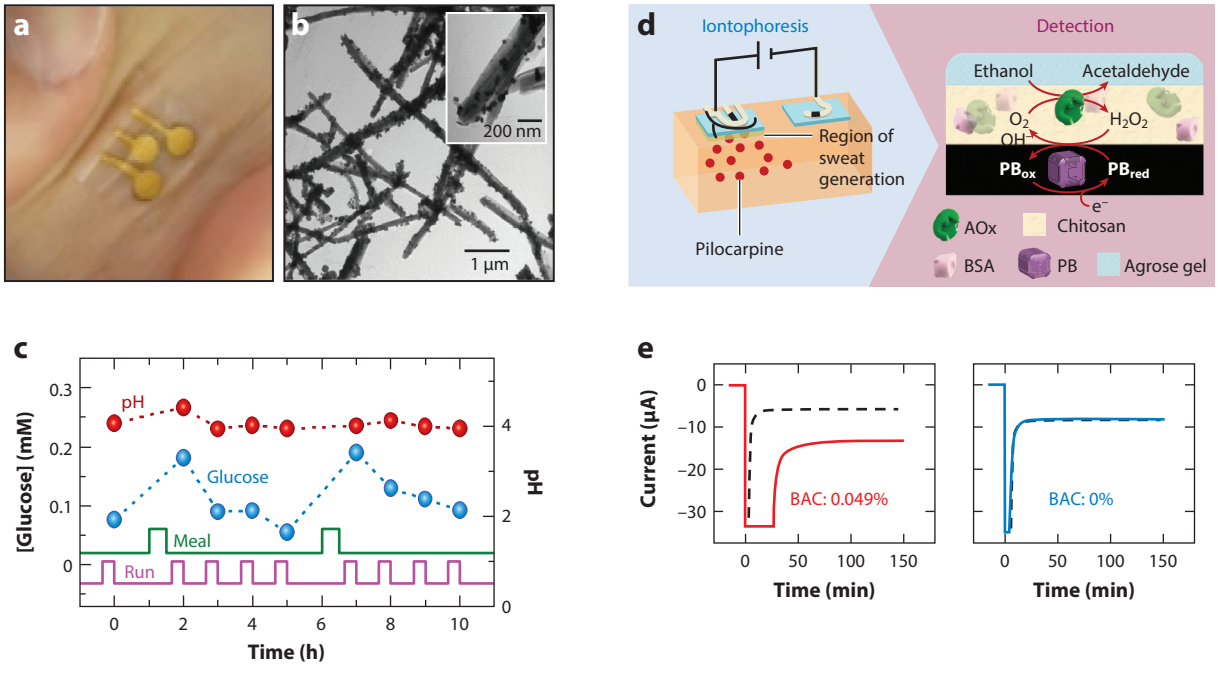

Figure 4

Wearable metabolic sensors. (*a*) Image of soft, stretchable gold nanosheet–based electrodes for electrochemical sensing. (*b*) Scanning electron microscope image of $CoWO_4$/CNTs. (*c*) Repeated measurement of sweat glucose by a $CoWO_4$/CNTs-based nonenzymatic sensor over several hours. Adapted with permission from Reference 90. Copyright 2018, American Chemical Society. (*d*) Schematic illustration of iontophoresis followed by electrochemical detection for sweat induction and quantification of sweat alcohol. (*e*) Data illustrating selectivity of the wearable alcohol sensor. Adapted with permission from Reference 85. Copyright 2016, American Chemical Society. Abbreviations: AOx, alcohol oxidase; BAC, blood alcohol concentration; BSA, bovine serum albumin; CNT, carbon nanotube; PB_{ox}, oxidized form of Prussian blue; PB_{red}, reduced form of Prussian blue.

[physiological range: 0.056–2.2 mM; median concentration: 0.17 mM (29)]. **Figure 4*c*** summarizes data from human trials that capture trends in measured glucose levels in response to exercise and meals.

In all cases, reliance on natural sweat generation associated with physical activity and/or exposure to hot, humid environments represents a limitation for certain applications such as those in intensive care and neonatal or pediatric monitoring. A widely adopted solution involves localized sweat generation via iontophoretic transdermal delivery of sweat-inducing drugs such as acetylcholine, pilocarpine, bethanechol, methacholine, and carbachol (94). Wearable devices that utilize this mechanism position sensing components between a pair of electrodes coated with stimulant-laden gel for iontophoresis. Examples include devices that detect sweat glucose (79) and alcohol (85). An alcohol monitoring sensor uses screen-printed Prussian blue on carbon and Ag/AgCl inks for base electrodes on a temporary tattoo substrate. Alcohol oxidase in agarose hydrogel and pilocarpine-saturated polyvinyl alcohol (PVA) functionalize the working electrode and positive iontophoretic electrode, respectively. A wireless electronics control module provides a fixed current (0.6 mA) across the iontophoretic electrodes to drive pilocarpine into the skin and induce local sweating. After 5 min, the module deactivates the iontophoresis process and activates the amperometric chemical sensor to detect alcohol levels in the released sweat (**Figure 4*d***). Human studies indicate promise for monitoring alcohol consumption in this manner (**Figure 4*e***).

3.2. Electrolytes

Electrolytes are critically important to several key physicochemical functions, such as active membrane transport, hydration, osmotic balance, nerve transduction, muscle activation, and many others. In extreme cases, electrolyte imbalance can lead to symptoms, including coma, seizures, and cardiac arrest. Hence, electrolytes represent the most widely targeted biomarkers in sweat analytics research. Examples of cations detected using potentiometric approaches include sodium (80), potassium (53), calcium (95), ammonium (96), and hydronium ions (97). Such sensors typically conformally coated drop-cast membranes of polyvinyl chloride (PVC) that incorporate selective ionophores and plasticizers to impart selectivity to indicator electrodes. Solid-state Ag/AgCl reference electrodes coated with polyvinyl butyral (PVB) saturated with sodium chloride are commonly used (98). Other sensors rely on chloride-containing printable ink (99, 100) and hydrogels of polyvinyl acetate (100) and poly (2-hydroxyethyl methacrylate) (101). A representative example of a wearable sweat sodium sensor is shown in **Figure 5*a***, which also includes onboard electronics for wireless data transmission (80). Here, the screen-printed working electrode derives its selectivity from a PVC cocktail solution that contains a sodium selective ionophore (4-*tert*-butylcalix[4]arene-tetraacetic acid tetraethyl ester), an ionic additive (sodium tetrakis[3,5-*bis*(trifluoromethyl)phenyl]borate), and a plasticizer [*bis*(2-ethylhexyl) sebacate]. Human field trials conducted during cycling demonstrate the practical utility of this skin-interfaced system in uncontrolled environments (**Figure 5*b***).

Figure 5*c* shows another wearable sensor that applies potentiometric detection of calcium and pH (95). The calcium-ion sensor utilizes a similar PVC-based indicator electrode coupled with a PVB-based Ag/AgCl reference. The pH indicator electrode leverages electrochemical synthesis of pH-sensitive polyaniline films for hydronium ion detection. Comparisons between on-body sensor data and ex situ sweat analysis [pH meter and inductively coupled plasma mass spectroscopy (ICP-MS)] reveal capabilities required for accurate measurements (**Figure 5*d***).

A unique colorimetric platform for measuring sweat pH takes the form of a fabric wristband infused with pH-sensitive dyes (methyl red, bromophenol blue, bromocresol green, bromocresol purple, and bromothymol blue) encapsulated in ionogels (trihexyltetradecylphosphonium

Cations

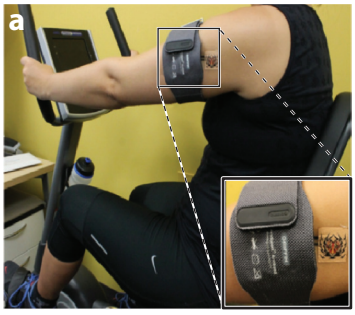

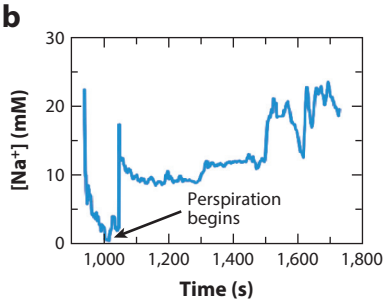

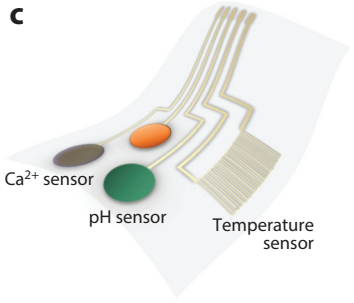

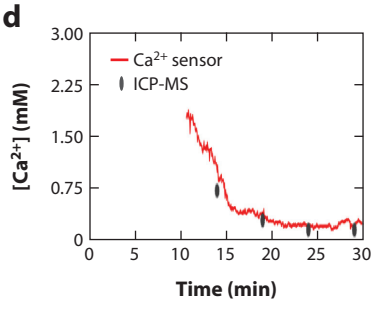

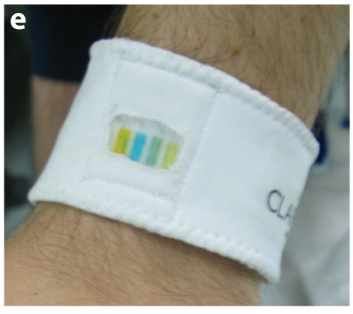

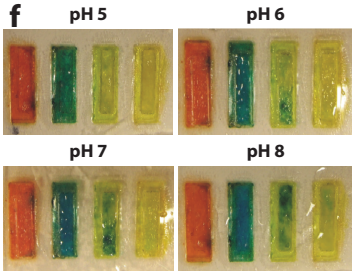

Anions

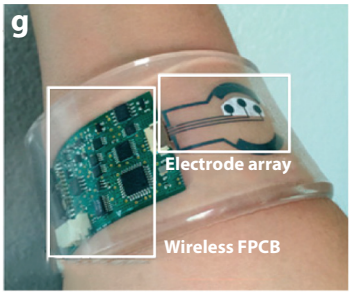

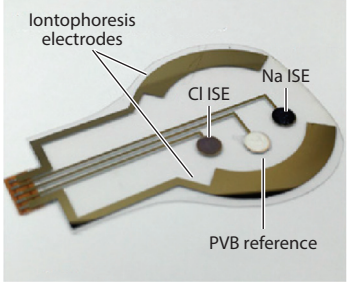

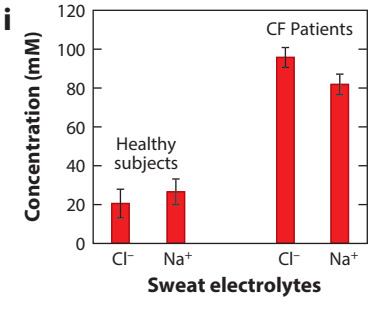

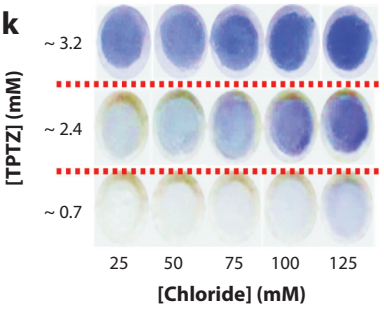

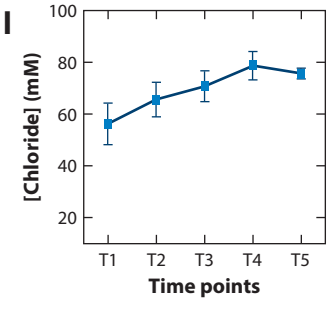

(*Caption appears on following page*)

Figure 5 (*Figure appears on preceding page*)

Wearable electrolytic sensors. (*a*) Image of a subject wearing a wireless BLE-based sodium sensor. (*b*) Real-time sweat sodium concentration recorded by the sweat sensor. Adapted with permission from Reference 80. Copyright 2014, Elsevier. (*c*) Image of a flexible wearable potentiometric sweat calcium and pH sensor. (*d*) Comparison of sweat calcium concentration variation with time acquired using the wearable sensor and ICP-MS. Adapted with permission from Reference 95. Copyright 2016, American Chemical Society. (*e*) Photograph of an ionogel-based colorimetric pH sensor embedded within a wristband. (*f*) Dependence of color of the ionogels on pH. Adapted with permission from Reference 97. Copyright 2012, Elsevier. (*g*) A subject wearing a flexible BLE-based iontophoretic/potentiometric system for sweat induction and sensing. (*h*) Image of the different electrodes in the chemical sensor. (*i*) Sweat chloride and sodium levels recorded from healthy and cystic fibrosis patients using the wearable sensor. Adapted with permission from Reference 79. Copyright 2017, PNAS. (*j*) Image of a microfluidic sweat sensor for time-sequenced colorimetric sampling of sweat chloride. (*k*) Evolution of chloride assay as a function of TPTZ and chloride concentration. (*l*) Data illustrating real-time variation in sweat chloride as recorded by the sweat-sensing patch. Adapted with permission from Reference 47. Copyright 2018, Wiley. Abbreviations: BLE, bluetooth low energy; CF, cystic fibrosis; FPCB, flexible printed circuit board; ICP-MS, inductively coupled plasma mass spectrometry; ISE, ion-selective electrode; PVB, polyvinyl butyral; TPTZ, 2,4,6-tris(2-pyridyl)-*s*-triazine.

dicyanamide in acrylamide polymer) (**Figure 5*e,f***) (97). The absorbent textile material wicks sweat from the skin, while the ionogel material minimizes evaporation due to its low vapor pressure. The wristband incorporates color reference markers that create a robust colorimetric pH barcode system.

Chloride is an important anion with significance in screening cystic fibrosis patients and monitoring electrolyte imbalance during sweating. One example uses an iontophoretic/sensing platform for sweat induction and subsequent potentiometric detection of sweat chloride for the former application (**Figure 5*g***) (79). The platform incorporates microfabricated iontophoretic electrodes for localized sweat stimulation and a solid-state potentiometric chloride sensor (**Figure 5*h***). Studies in healthy populations and those with cystic fibrosis illustrate the potential of this technology as a point-of-care tool for screening (**Figure 5*i***). Colorimetric approaches offer simple yet robust alternatives, as demonstrated in an assay that consists of 2,4,6-tris(2-pyridyl)-*s*-triazine (TPTZ, a chelating agent), Hg^{2+}, and Fe^{2+} (**Figure 5*j***) (47). TPTZ preferentially complexes with Hg^{2+} to form colorless $Hg[TPTZ]_2$. Chloride ions readily react with the complex to produce mercuric chloride, $HgCl_2$. Hence, introduction of chloride results in a proportional release of TPTZ, which then chelates with the Fe^{2+} to form blue $Fe[TPTZ]_2$ (**Figure 5*k***). Measuring the resulting blue intensity thus provides a colorimetric method for measuring chloride. **Figure 5*l*** highlights data from human trials showing that chloride levels could fluctuate during exercise.

3.3. Multimodal and Multianalyte Sensing Platforms

Recent developments in multianalyte sensing platforms allow for cross comparisons of sweat biomarkers, providing enhanced, comprehensive evaluation of health status. **Figure 6*a*** shows an electrochemical multianalyte sensing system that relies on various enzyme-based and ion-selective microfabricated electrodes deposited on a flexible PET sheet (53). This system supports amperometric detection of glucose and lactate and potentiometric detection of chloride, sodium, and potassium. In addition, a resistive temperature sensor compensates for fluctuations in temperature. On-body trials involve participants cycling while sensors instrumented on each subject's forehead transmit real-time data wirelessly to a smartphone.

Recent reports introduce the use of colorimetric strategies in skin-interfaced microfluidic systems for ultralightweight battery-free multianalyte sensing. In one example, microfluidic channels route sweat to multianalyte wells and reservoirs preloaded with chemical and enzymatic assays for assessment of biomarker concentrations (glucose, lactate, chloride, and pH) and to a separate serpentine microchannel for measurement of sweat rate and instantaneous total sweat loss (46). The

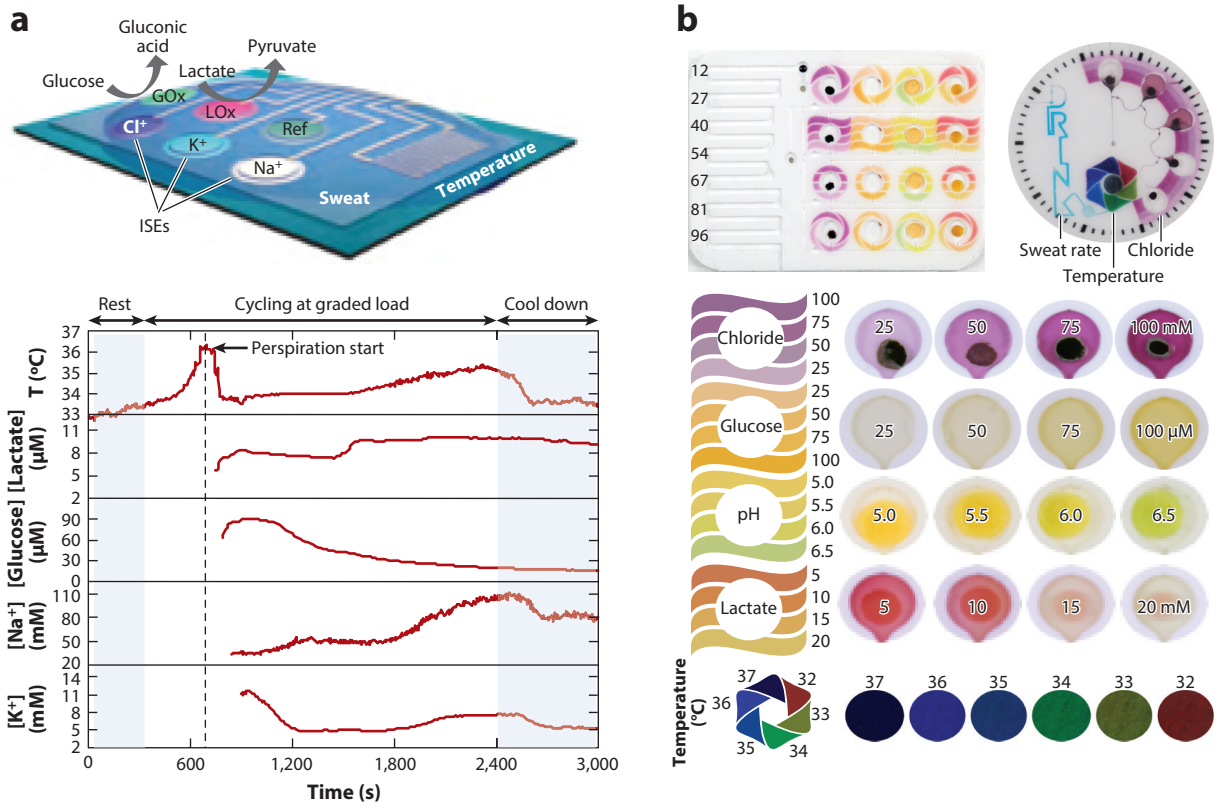

Figure 6

Multimodal and multianalyte sensing platforms. (*a*) Electrochemical and (*b*) colorimetric platforms for multianalyte sweat sensing. Panel *a* adapted with permission from Reference 53, copyright 2016, Springer Nature; panel *b* adapted with permission from Reference 48, copyright 2018, AAAS. Abbreviation: ISE, ion-selective electrode.

enzyme-based colorimetric assays use lactate dehydrogenase and diaphorase and glucose oxidase for selective detection of lactate and glucose, respectively. Colorimetric readouts of chloride and pH levels follow from reactions with TPTZ and a commercial pH paper, respectively. Advanced platforms of this general type combine microfluidic channels with integrated arrays of CBVs (discussed in Section 2.3) that connect with individual microfluidic channels for chrono-sampling of sweat (48). The microchannels route sweat to colorimetric assay chambers for time-sequenced detection of sweat glucose, lactate, chloride, and pH in this demonstration (**Figure 6*b***). In addition to the multianalyte biomarker analyzer this CBV-based microfluidic device contains a thermochromic liquid crystal temperature sensor and a long, meandering channel with a water-soluble dye near the inlet for visualization of sweat rate and loss. The system operates in a purely passive mode without bulky power sources or electronics/actuators. This operation results in a drastic reduction in device footprint, cost, and potential points of mechanical failure.

3.4. Other Targets

Despite widely recognized adverse health effects of heavy metals, these environmental pollutants remain a significant health concern in developed and developing countries alike. Monitoring

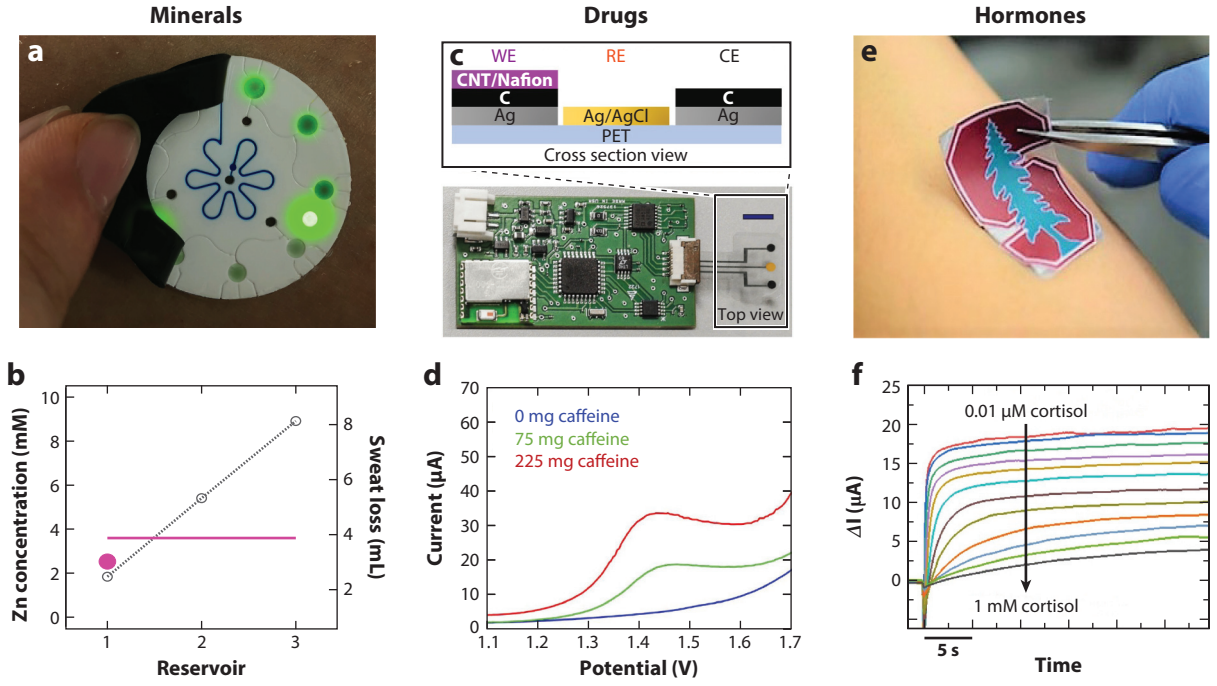

Figure 7

Wearable sensors for other targets. (*a*) Image of a wearable fluorometric microfluidic system for measuring sweat zinc, sodium, and chloride concentrations in addition to sweat loss. (*b*) Variation of sweat zinc concentration and sweat loss measured by the device. Adapted with permission from Reference 49. Copyright 2018, Royal Society of Chemistry. (*c*) Schematic illustration and image of a BLE-based voltammetric sensor for measuring caffeine in sweat. (*d*) Voltammetric response as a function of caffeine consumed by a human subject. Adapted with permission from Reference 105. Copyright 2018, Wiley. (*e*) Image of a field-effect transistor-based wearable cortisol sensor. (*f*) Sensor response to increasing cortisol concentration. Adapted with permission from Reference 88. Copyright 2018, AAAS. Abbreviations: BLE, bluetooth low energy; CE, counter electrode; CNT, carbon nanotube; PET, polyethylene terephthalate; RE, reference electrode; WE, working electrode.

of such toxins through sweat excretion represents a unique, unconventional route for rapid screening of pollutant exposure. Moreover, studies have found correlations between the presence of heavy metals in sweat and athletic endurance and recovery (102). One electrochemical approach facilitates heavy metal detection in sweat through stripping voltammetry-based techniques (103, 104). Carbon or gold electrodes layered with bismuth and tetrafluoroethylene-perfluoro-3,6-dioxa-4-methyl-7-octenesulfonic acid copolymer provide low-toxicity alternatives to conventional mercury-coated electrodes. Detection occurs by (1) electrodeposition of heavy metal analytes and (2) stripping of the metals to yield distinct voltammetric oxidation peaks for each analyte (e.g., copper, cadmium, zinc, arsenic). This approach yields limits of detection in parts per million and up to parts per trillion.

Another approach leverages fluorophores embedded in skin-interfaced microfluidic systems and a plug-in module attached to a smartphone, as the basis of a fluorescence-based scheme for detection of sweat zinc, sodium, and chloride (**Figure 7*a*,*b***) (49). Fluorescent assays in sequential reaction chambers react to generate fluorescent signals that are proportional to analyte concentrations. Cations are detected via commercially available fluorescent assays while the chloride assay exploits the diffusion-limited collisional quenching of bis-*N*-methylacridinium nitrate in the presence of chloride. Reaction chambers containing known quantities of dyes provide reference

readings. A smartphone camera attachment facilitates convenient in situ excitation, detection, and analysis.

A method similar to voltammetric heavy metal detection can be applied to quantifying the concentrations of certain drugs in sweat, as recently illustrated (**Figure 7*c*,*d***) (105). The device combines iontophoretic components for sweat generation and a caffeine (a representative drug) sensing system that uses a CNT-coated carbon working electrode, a bare carbon counter electrode, and a silver/silver chloride reference electrode. Human trials reveal a linear increase in sensor signal with the volume of coffee consumed.

Hormones represent an interesting class of small molecules with relevance across a broad range of physiological functions. For example, several studies have established a correlation between cortisol levels and stress (106, 107). A recent study exploits a stretchable styrene-ethylene-butylene-styrene elastomer substrate with molecularly imprinted polymer (MIP) for conductometry-based detection of cortisol in sweat (**Figure 7*e*,*f***) (88). A layer of poly(3,4-ethylenedioxythiophene) polystyrene sulfonate (PEDOT:PSS) functions as an organic transistor with an Ag/AgCl gate coated by acrylate-based MIP for cortisol selectivity. Binding of cortisol to the MIP-functionalized gate electrode causes a change in conductance. This allows for cortisol measurements by monitoring modulations in drain current. Benchtop studies reveal a linear response to increasing cortisol concentrations down to 10 nM.

4. GRAND CHALLENGES FOR FUTURE RESEARCH

Despite these substantial advancements in wearable chemical sweat sensors, several challenges remain in aspects related to operation, stability, sensitivity, selectivity, biofouling, and power supply (108). For example, potentiometric sensors require calibration procedures, storage in conditioning solutions, and other operations that are poorly suited for wearable platforms. Additionally, field deployment of these devices requires stable, predictable responses across a wide range of temperatures, sweat compositions, sunlight exposure levels, and other factors that may affect signal response. These variabilities are particularly significant because the concentrations of important analytes in sweat are often extremely low. Here, noise from contamination and interfering species could further degrade performance. Traditional biosensors circumvent these issues by exploiting multistep sensing mechanisms to detect ultralow analyte levels and sample pretreatments to improve selectivity. Such techniques are, however, incompatible with wearable devices that must sample sweat directly from the skin and perform real-time, in situ analysis. Hence, novel electrochemical sensing protocols and colorimetric chemistries for highly sensitive, selective sweat sensing that are optimized for stable wearable operation under various environmental conditions present a prominent area for improvement.

Equally daunting challenges exist in technologies for continuously powering wearable chemical sensors. Most devices employ commercial coin cell batteries, in spite of their weight, bulk, and rigid mechanical properties. Flexible batteries have some potential in this context but at significant additional cost. Research examples of wearable flexible/stretchable batteries are of interest, but most have inferior performance characteristics. Battery-free strategies based on wireless power transfer using NFC technologies are promising but require close proximity (up to ~1 m) to a transmission antenna for continuous data acquisition. Ultimately, streamlined cointegration of the various subsystems needed in a wearable sweat sensor remains an overarching technological hurdle. Difficulties largely follow from disparate fabrication processes, materials, and encapsulations needed for various active and passive components. For example, chemical sensors must remain in direct contact with sweat, while supporting electronics must be completely sealed from any biofluid or moisture exposure. From a practical standpoint, the interfaces between different

sensor components often experience mechanical failure. Thus, sophisticated packaging strategies for robust integration of heterogeneous subsystems represent an important area for future work.

5. CONCLUSIONS

Research in flexible/stretchable materials, solid-state electrode micro-/nanostructures and soft, skin-interfaced microfluidics technologies form the basis of recent advances in the field of wearable sweat sensing. These emerging systems support important functions that complement those of biophysical sensors found in mature wearable platforms. The results of combined biochemical and biophysical measurements have the potential to yield a comprehensive set of insights into physiological health. Demonstrated examples of wearable chemical sensors offer promising, practical capabilities in monitoring of metabolites, electrolytes, heavy metals, drugs, and hormones. Additional work will expand the sensing modalities, accuracy, and robustness of these systems. Broad ranges of interesting topics in materials science, analytical chemistry, electrical and mechanical engineering, clinical medicine, and fitness support diverse opportunities for fundamental and applied research. Successful outcomes could have a profound, positive effect on the ubiquity, efficiency, cost, and efficacy of health monitoring and individualized patient care.

DISCLOSURE STATEMENT

R.G. is co-founder of Epicore Biosystems, Inc., which is pursuing commercialization of wearable microfluidic devices. J.A.R. is involved as co-founder of an early commercial development of skin-mounted sweat sensors. The remaining authors are not aware of any affiliations, memberships, funding, or financial holdings that might be perceived as affecting the objectivity of this review.

ACKNOWLEDGMENTS

This work was supported by the Center for Bio-Integrated Electronics of the Simpson Querrey Institute for BioNanotechnology.

LITERATURE CITED

1. Rogers JA, Someya T, Huang Y. 2010. Materials and mechanics for stretchable electronics. *Science* 327(5973):1603–7
2. Heikenfeld J, Jajack A, Rogers J, Gutruf P, Tian L, et al. 2018. Wearable sensors: modalities, challenges, and prospects. *Lab Chip* 18(2):217–48
3. Bandodkar AJ, Wang J. 2014. Non-invasive wearable electrochemical sensors: a review. *Trends Biotechnol.* 32(7):363–71
4. Choi S, Lee H, Ghaffari R, Hyeon T, Kim D-H. 2016. Recent advances in flexible and stretchable bio-electronic devices integrated with nanomaterials. *Adv. Mater.* 28(22):4203–18
5. Bao Z, Chen X. 2016. Flexible and stretchable devices. *Adv. Mater.* 28(22):4177–79
6. Someya T, Bao Z, Malliaras GG. 2016. The rise of plastic bioelectronics. *Nature* 540(7633):379–85
7. Ryu S, Lee P, Chou JB, Xu R, Zhao R, et al. 2015. Extremely elastic wearable carbon nanotube fiber strain sensor for monitoring of human motion. *ACS Nano* 9(6):5929–36
8. Pawar T, Chaudhuri S, Duttagupta SP. 2007. Body movement activity recognition for ambulatory cardiac monitoring. *IEEE Trans. Biomed. Eng.* 54(5):874–82
9. Trung TQ, Ramasundaram S, Hwang B-U, Lee N-E. 2016. An all-elastomeric transparent and stretchable temperature sensor for body-attachable wearable electronics. *Adv. Mater.* 28(3):502–9

10. Krishnan S, Shi Y, Webb RC, Ma Y, Bastien P, et al. 2017. Multimodal epidermal devices for hydration monitoring. *Microsyst. Nanoeng.* 3:17014
11. Kim T, Park J, Sohn J, Cho D, Jeon S. 2016. Bioinspired, highly stretchable, and conductive dry adhesives based on 1D–2D hybrid carbon nanocomposites for all-in-one ECG electrodes. *ACS Nano* 10(4):4770–78
12. Jeong JW, Kim MK, Cheng H, Yeo WH, Huang X, et al. 2014. Capacitive epidermal electronics for electrically safe, long-term electrophysiological measurements. *Adv. Healthc. Mater.* 3(5):642–48
13. Liu Y, Pharr M, Salvatore GA. 2017. Lab-on-skin: a review of flexible and stretchable electronics for wearable health monitoring. *ACS Nano* 11(10):9614–35
14. Xu S, Zhang Y, Jia L, Mathewson KE, Jang K-I, et al. 2014. Soft microfluidic assemblies of sensors, circuits, and radios for the skin. *Science* 344(6179):70–74
15. Kim D-H, Lu N, Ma R, Kim Y-S, Kim R-H, et al. 2011. Epidermal electronics. *Science* 333(6044):838–43
16. Tian L, Li Y, Webb RC, Krishnan S, Bian Z, et al. 2017. Flexible and stretchable 3ω sensors for thermal characterization of human skin. *Adv. Funct. Mater.* 27(26):1701282
17. Chiang PY, Chao PCP, Tarng DC, Yang CY. 2017. A novel wireless photoplethysmography blood-flow volume sensor for assessing arteriovenous fistula of hemodialysis patients. *IEEE Trans. Ind. Electron.* 64(12):9626–35
18. Higurashi E, Sawada R, Ito T. 2003. An integrated laser blood flowmeter. *J. Lightwave Technol.* 21(3):591–95
19. Heikenfeld J. 2016. Non-invasive analyte access and sensing through eccrine sweat: challenges and outlook circa 2016. *Electroanalysis* 28(6):1242–49
20. Mena-Bravo A, Luque de Castro MD. 2014. Sweat: a sample with limited present applications and promising future in metabolomics. *J. Pharm. Biomed. Anal.* 90:139–47
21. Calderón-Santiago M, Priego-Capote F, Turck N, Robin X, Jurado-Gámez B, et al. 2015. Human sweat metabolomics for lung cancer screening. *Anal. Bioanal. Chem.* 407(18):5381–92
22. Adewole OO, Erhabor GE, Adewole TO, Ojo AO, Oshokoya H, et al. 2016. Proteomic profiling of eccrine sweat reveals its potential as a diagnostic biofluid for active tuberculosis. *Proteom. Clin. Appl.* 10(5):547–53
23. Hammond KB, Turcios NL, Gibson LE. 1994. Clinical evaluation of the macroduct sweat collection system and conductivity analyzer in the diagnosis of cystic fibrosis. *J. Pediatr.* 124(2):255–60
24. Wang J. 2005. Carbon-nanotube based electrochemical biosensors: a review. *Electroanalysis* 17(1):7–14
25. Biju V. 2014. Chemical modifications and bioconjugate reactions of nanomaterials for sensing, imaging, drug delivery and therapy. *Chem. Soc. Rev.* 43(3):744–64
26. Matharu Z, Bandodkar AJ, Gupta V, Malhotra BD. 2012. Fundamentals and application of ordered molecular assemblies to affinity biosensing. *Chem. Soc. Rev.* 41(3):1363–402
27. Matharu Z, Daggumati P, Wang L, Dorofeeva TS, Li Z, Seker E. 2017. Nanoporous-gold-based electrode morphology libraries for investigating structure–property relationships in nucleic acid based electrochemical biosensors. *ACS Appl. Mater. Interfaces* 9(15):12959–66
28. Kidwell DA, Holland JC, Athanaselis S. 1998. Testing for drugs of abuse in saliva and sweat. *J. Chromatogr. B Biomed. Sci. Appl.* 713(1):111–35
29. Harvey CJ, LeBouf RF, Stefaniak AB. 2010. Formulation and stability of a novel artificial human sweat under conditions of storage and use. *Toxicol. In Vitro* 24(6):1790–96
30. Bobacka J. 1999. Potential stability of all-solid-state ion-selective electrodes using conducting polymers as ion-to-electron transducers. *Anal. Chem.* 71(21):4932–37
31. Crespo GA, Macho S, Rius FX. 2008. Ion-selective electrodes using carbon nanotubes as ion-to-electron transducers. *Anal. Chem.* 80(4):1316–22
32. Li H, Smart RB. 1996. Determination of sub-nanomolar concentration of arsenic (III) in natural waters by square wave cathodic stripping voltammetry. *Anal. Chim. Acta* 325(1–2):25–32
33. Jiokeng SL, Dongmo LM, Ymélé E, Ngameni E, Tonlé IK. 2017. Sensitive stripping voltammetry detection of Pb(II) at a glassy carbon electrode modified with an amino-functionalized attapulgite. *Sens. Actuators B* 242:1027–34

34. Bandodkar AJ, O'Mahony AM, Ramírez J, Samek IA, Anderson SM, et al. 2013. Solid-state *Forensic Finger* sensor for integrated sampling and detection of gunshot residue and explosives: towards 'lab-on-a-finger'. *Analyst* 138(18):5288–95
35. Sanghavi BJ, Wolfbeis OS, Hirsch T, Swami NS. 2015. Nanomaterial-based electrochemical sensing of neurological drugs and neurotransmitters. *Microchim. Acta* 182(1–2):1–41
36. Izadyar A, Arachchige DR, Cornwell H, Hershberger JC. 2016. Ion transfer stripping voltammetry for the detection of nanomolar levels of fluoxetine, citalopram, and sertraline in tap and river water samples. *Sens. Actuators B* 223:226–33
37. De Jong M, Sleegers N, Kim J, Van Durme F, Samyn N, et al. 2016. Electrochemical fingerprint of street samples for fast on-site screening of cocaine in seized drug powders. *Chem. Sci.* 7(3):2364–70
38. Mishra RK, Hubble LJ, Martín A, Kumar R, Barfidokht A, et al. 2017. Wearable flexible and stretchable glove biosensor for on-site detection of organophosphorus chemical threats. *ACS Sens.* 2(4):553–61
39. Gupta BD, Shrivastav AM, Usha SP. 2017. *Optical Sensors for Biomedical Diagnostics and Environmental Monitoring*. Boca Raton, FL: CRC Press
40. Caucheteur C, Guo T, Albert J. 2015. Review of plasmonic fiber optic biochemical sensors: improving the limit of detection. *Anal. Bioanal. Chem.* 407(14):3883–97
41. Verma R, Gupta BD. 2015. Detection of heavy metal ions in contaminated water by surface plasmon resonance based optical fibre sensor using conducting polymer and chitosan. *Food Chem.* 166:568–75
42. Gillanders RN, Samuel ID, Turnbull GA. 2017. A low-cost, portable optical explosive-vapour sensor. *Sens. Actuators B* 245:334–40
43. Zhu H, Fan J, Wang B, Peng X. 2015. Fluorescent, MRI, and colorimetric chemical sensors for the first-row d-block metal ions. *Chem. Soc. Rev.* 44(13):4337–66
44. Du Y, Guo S. 2016. Chemically doped fluorescent carbon and graphene quantum dots for bioimaging, sensor, catalytic and photoelectronic applications. *Nanoscale* 8(5):2532–43
45. Polavarapu L, Pérez-Juste J, Xu Q-H, Liz-Marzán LM. 2014. Optical sensing of biological, chemical and ionic species through aggregation of plasmonic nanoparticles. *J. Mater. Chem. C* 2(36):7460–76
46. Koh A, Kang D, Xue Y, Lee S, Pielak RM, et al. 2016. A soft, wearable microfluidic device for the capture, storage, and colorimetric sensing of sweat. *Sci. Transl. Med.* 8(366):366ra165
47. Kim SB, Zhang Y, Won SM, Bandodkar AJ, Sekine Y, et al. 2018. Super-absorbent polymer valves and colorimetric chemistries for time-sequenced discrete sampling and chloride analysis of sweat via skin-mounted soft microfluidics. *Small* 14(12):1703334
48. Choi J, Ghaffari R, Baker LB, Rogers JA. 2018. Skin-interfaced systems for sweat collection and analytics. *Sci. Adv.* 4(2):eaar3921
49. Sekine Y, Kim SB, Zhang Y, Bandodkar AJ, Xu S, et al. 2018. A fluorometric skin-interfaced microfluidic device and smartphone imaging module for in situ quantitative analysis of sweat chemistry. *Lab Chip* 18(15):2178–86
50. Wang C, Wang C, Huang Z, Xu S. 2018. Materials and structures toward soft electronics. *Adv. Mater.* 30(50):1801368
51. Imani S, Bandodkar AJ, Mohan AMV, Kumar R, Yu S, et al. 2016. A wearable chemical–electrophysiological hybrid biosensing system for real-time health and fitness monitoring. *Nat. Commun.* 7:11650
52. Nakata S, Arie T, Akita S, Takei K. 2017. Wearable, flexible, and multifunctional healthcare device with an ISFET chemical sensor for simultaneous sweat pH and skin temperature monitoring. *ACS Sens.* 2(3):443–48
53. Gao W, Emaminejad S, Nyein HYY, Challa S, Chen K, et al. 2016. Fully integrated wearable sensor arrays for multiplexed *in situ* perspiration analysis. *Nature* 529:509
54. Bandodkar AJ, Jia W, Yardımcı C, Wang X, Ramirez J, Wang J. 2014. Tattoo-based noninvasive glucose monitoring: a proof-of-concept study. *Anal. Chem.* 87(1):394–98
55. Bandodkar AJ, Jia W, Wang J. 2015. Tattoo-based wearable electrochemical devices: a review. *Electroanalysis* 27(3):562–72
56. Castano LM, Flatau AB. 2014. Smart fabric sensors and e-textile technologies: a review. *Smart Mater. Struct.* 23(5):053001

57. Parrilla M, Cánovas R, Jeerapan I, Andrade FJ, Wang J. 2016. A textile-based stretchable multi-ion potentiometric sensor. *Adv. Healthc. Mater.* 5(9):996–1001
58. Caldara M, Colleoni C, Guido E, Re V, Rosace G. 2016. Optical monitoring of sweat pH by a textile fabric wearable sensor based on covalently bonded litmus-3-glycidoxypropyltrimethoxysilane coating. *Sens. Actuators B* 222:213–20
59. Windmiller JR, Bandodkar AJ, Parkhomovsky S, Wang J. 2012. Stamp transfer electrodes for electrochemical sensing on non-planar and oversized surfaces. *Analyst* 137(7):1570–75
60. Liu X, Lillehoj PB. 2016. Embroidered electrochemical sensors for biomolecular detection. *Lab Chip* 16(11):2093–98
61. Jeerapan I, Sempionatto JR, Pavinatto A, You J-M, Wang J. 2016. Stretchable biofuel cells as wearable textile-based self-powered sensors. *J. Mater. Chem. A* 4(47):18342–53
62. Bandodkar AJ, Jeerapan I, You J-M, Nuñez-Flores R, Wang J. 2015. Highly stretchable fully-printed CNT-based electrochemical sensors and biofuel cells: combining intrinsic and design-induced stretchability. *Nano Lett.* 16(1):721–27
63. Bell CA, Yu J, Barker IA, Truong VX, Cao Z, et al. 2016. Independent control of elastomer properties through stereocontrolled synthesis. *Angew. Chem. Int. Ed.* 55(42):13076–80
64. Kojio K, Fukumaru T, Furukawa M. 2004. Highly softened polyurethane elastomer synthesized with novel 1,2-bis(isocyanate)ethoxyethane. *Macromolecules* 37(9):3287–91
65. Jang K-I, Chung HU, Xu S, Lee CH, Luan H, et al. 2015. Soft network composite materials with deterministic and bio-inspired designs. *Nat. Commun.* 6:6566
66. Wilke K, Martin A, Terstegen L, Biel S. 2007. A short history of sweat gland biology. *Int. J. Cosmet. Sci.* 29(3):169–79
67. Taylor NA, Machado-Moreira CA. 2013. Regional variations in transepidermal water loss, eccrine sweat gland density, sweat secretion rates and electrolyte composition in resting and exercising humans. *Extreme Physiol. Med.* 2(1):4
68. Roberts MF, Wenger CB, Stolwijk J, Nadel ER. 1977. Skin blood flow and sweating changes following exercise training and heat acclimation. *J. Appl. Physiol.* 43(1):133–37
69. Anderson RK, Kenney WL. 1987. Effect of age on heat-activated sweat gland density and flow during exercise in dry heat. *J. Appl. Physiol.* 63(3):1089–94
70. Kim T-W, Shin Y-O, Lee J-B, Min Y-K, Yang H-M. 2010. Effect of caffeine on the metabolic responses of lipolysis and activated sweat gland density in human during physical activity. *Food Sci. Biotechnol.* 19(4):1077–81
71. Adams WC, Mack GW, Langhans GW, Nadel ER. 1992. Effects of varied air velocity on sweating and evaporative rates during exercise. *J. Appl. Physiol.* 73(6):2668–74
72. Allen JA, Armstrong JE, Roddie I. 1973. The regional distribution of emotional sweating in man. *J. Physiol.* 235(3):749–59
73. Gibson LE, Cooke RE. 1959. A test for concentration of electrolytes in sweat in cystic fibrosis of the pancreas utilizing pilocarpine by iontophoresis. *Pediatrics* 23(3):545–49
74. Nge PN, Rogers CI, Woolley AT. 2013. Advances in microfluidic materials, functions, integration, and applications. *Chem. Rev.* 113(4):2550–83
75. Nyein HYY, Tai L-C, Ngo QP, Chao M, Zhang G, et al. 2018. A wearable sweat sensing patch for dynamic sweat secretion analysis. *ACS Sens.* 3(5):944–52
76. Martín A, Kim J, Kurniawan JF, Sempionatto JR, Moreto JR, et al. 2017. Epidermal microfluidic electrochemical detection system: enhanced sweat sampling and metabolite detection. *ACS Sens.* 2(12):1860–68
77. Choi J, Kang D, Han S, Kim SB, Rogers JA. 2017. Thin, soft, skin-mounted microfluidic networks with capillary bursting valves for chrono-sampling of sweat. *Adv. Healthc. Mater.* 6(5):1601355
78. Choi J, Xue Y, Xia W, Ray TR, Reeder JT, et al. 2017. Soft, skin-mounted microfluidic systems for measuring secretory fluidic pressures generated at the surface of the skin by eccrine sweat glands. *Lab Chip* 17(15):2572–80
79. Emaminejad S, Gao W, Wu E, Davies ZA, Nyein HYY, et al. 2017. Autonomous sweat extraction and analysis applied to cystic fibrosis and glucose monitoring using a fully integrated wearable platform. *PNAS* 114(18):4625–30

80. Bandodkar AJ, Molinnus D, Mirza O, Guinovart T, Windmiller JR, et al. 2014. Epidermal tattoo potentiometric sodium sensors with wireless signal transduction for continuous non-invasive sweat monitoring. *Biosens. Bioelectron.* 54(Suppl. C):603–9
81. Rose DP, Ratterman ME, Griffin DK, Hou L, Kelley-Loughnane N, et al. 2015. Adhesive RFID sensor patch for monitoring of sweat electrolytes. *IEEE Trans. Biomed. Eng.* 62(6):1457–65
82. Kim J, Campbell AS, Wang J. 2018. Wearable non-invasive epidermal glucose sensors: a review. *Talanta* 177(Suppl. C):163–70
83. Abellán-Llobregat A, Jeerapan I, Bandodkar A, Vidal L, Canals A, et al. 2017. A stretchable and screen-printed electrochemical sensor for glucose determination in human perspiration. *Biosens. Bioelectron.* 91:885–91
84. Lee H, Hong YJ, Baik S, Hyeon T, Kim DH. 2018. Enzyme-based glucose sensor: from invasive to wearable device. *Adv. Healthc. Mater.* 7(8):1701150
85. Kim J, Jeerapan I, Imani S, Cho TN, Bandodkar A, et al. 2016. Noninvasive alcohol monitoring using a wearable tattoo-based iontophoretic-biosensing system. *ACS Sens.* 1(8):1011–19
86. Kim J, Sempionatto JR, Imani S, Hartel MC, Barfidokht A, et al. 2018. Simultaneous monitoring of sweat and interstitial fluid using a single wearable biosensor platform. *Adv. Sci.* 5(10):1800880
87. Schazmann B, Morris D, Slater C, Beirne S, Fay C, et al. 2010. A wearable electrochemical sensor for the real-time measurement of sweat sodium concentration. *Anal. Methods* 2(4):342–48
88. Parlak O, Keene ST, Marais A, Curto VF, Salleo A. 2018. Molecularly selective nanoporous membrane-based wearable organic electrochemical device for noninvasive cortisol sensing. *Sci. Adv.* 4(7):eaar2904
89. Jia W, Bandodkar AJ, Valdés-Ramírez G, Windmiller JR, Yang Z, et al. 2013. Electrochemical tattoo biosensors for real-time noninvasive lactate monitoring in human perspiration. *Anal. Chem.* 85(14):6553–60
90. Oh SY, Hong SY, Jeong YR, Yun J, Park H, et al. 2018. Skin-attachable, stretchable electrochemical sweat sensor for glucose and pH detection. *ACS Appl. Mater. Interfaces* 10(16):13729–40
91. Khodagholy D, Curto VF, Fraser KJ, Gurfinkel M, Byrne R, et al. 2012. Organic electrochemical transistor incorporating an ionogel as a solid state electrolyte for lactate sensing. *J. Mater. Chem.* 22(10):4440–43
92. Kim J, Kumar R, Bandodkar AJ, Wang J. 2017. Advanced materials for printed wearable electrochemical devices: a review. *Adv. Electron. Mater.* 3(1):1600260
93. Lee H, Choi TK, Lee YB, Cho HR, Ghaffari R, et al. 2016. A graphene-based electrochemical device with thermoresponsive microneedles for diabetes monitoring and therapy. *Nat. Nanotech.* 11(6):566–72
94. Simmers P, Li SK, Kasting G, Heikenfeld J. 2018. Prolonged and localized sweat stimulation by iontophoretic delivery of the slowly-metabolized cholinergic agent carbachol. *J. Dermatol. Sci.* 89(1):40–51
95. Nyein HYY, Gao W, Shahpar Z, Emaminejad S, Challa S, et al. 2016. A wearable electrochemical platform for noninvasive simultaneous monitoring of Ca^{2+} and pH. *ACS Nano* 10(7):7216–24
96. Guinovart T, Bandodkar AJ, Windmiller JR, Andrade FJ, Wang J. 2013. A potentiometric tattoo sensor for monitoring ammonium in sweat. *Analyst* 138(22):7031–38
97. Curto VF, Fay C, Coyle S, Byrne R, O'Toole C, et al. 2012. Real-time sweat pH monitoring based on a wearable chemical barcode micro-fluidic platform incorporating ionic liquids. *Sens. Actuators B* 171–172(Suppl. C):1327–34
98. Parrilla M, Ferré J, Guinovart T, Andrade FJ. 2016. Wearable potentiometric sensors based on commercial carbon fibres for monitoring sodium in sweat. *Electroanalysis* 28(6):1267–75
99. Bandodkar AJ, Hung VW, Jia W, Valdés-Ramírez G, Windmiller JR, et al. 2013. Tattoo-based potentiometric ion-selective sensors for epidermal pH monitoring. *Analyst* 138(1):123–28
100. Wang S, Wu Y, Gu Y, Li T, Luo H, et al. 2017. Wearable sweatband sensor platform based on gold nanodendrite array as efficient solid contact of ion-selective electrode. *Anal. Chem.* 89(19):10224–31
101. Gonzalo-Ruiz J, Mas R, de Haro C, Cabruja E, Camero R, et al. 2009. Early determination of cystic fibrosis by electrochemical chloride quantification in sweat. *Biosens. Bioelectron.* 24(6):1788–91
102. Speich M, Pineau A, Ballereau F. 2001. Minerals, trace elements and related biological variables in athletes and during physical activity. *Clin. Chim. Acta* 312(1–2):1–11
103. Gao W, Nyein HY, Shahpar Z, Fahad HM, Chen K, et al. 2016. Wearable microsensor array for multiplexed heavy metal monitoring of body fluids. *ACS Sens.* 1(7):866–74

104. Kim J, de Araujo WR, Samek IA, Bandodkar AJ, Jia W, et al. 2015. Wearable temporary tattoo sensor for real-time trace metal monitoring in human sweat. *Electrochem. Commun.* 51:41–45
105. Tai LC, Gao W, Chao M, Bariya M, Ngo QP, et al. 2018. Methylxanthine drug monitoring with wearable sweat sensors. *Adv. Mater.* 30(23):1707442
106. Heinrichs M, Baumgartner T, Kirschbaum C, Ehlert U. 2003. Social support and oxytocin interact to suppress cortisol and subjective responses to psychosocial stress. *Biol. Psychiatry* 54(12):1389–98
107. Russell E, Koren G, Rieder M, Van Uum SH. 2014. The detection of cortisol in human sweat: implications for measurement of cortisol in hair. *Ther. Drug Monit.* 36(1):30–34
108. Bandodkar AJ, Jeerapan I, Wang J. 2016. Wearable chemical sensors: present challenges and future prospects. *ACS Sens.* 1(5):464–82

Annual Review of
Analytical Chemistry

Volume 12, 2019

Contents

Errata

An online log of corrections to *Annual Review of Analytical Chemistry* articles may be found at http://www.annualreviews.org/errata/anchem